Anal. Chem. **2002,** *74,* 3348−3353

Dual Fluorescence and Electrochemical Detection on an Electrophoresis Microchip

Julie A. Lapos,† Drew P. Manica,† and Andrew G. Ewing*

152 Davey Laboratory, Department of Chemistry, Pennsylvania State University, University Park, Pennsylvania 16802

Simultaneous amperometric and fluorescence detection in a microfabricated electrophoresis chip is reported. Detection limits of 448 nM and 1.52, 16, and 28 μM have been achieved for dopamine, catechol, NBD−arginine, and NBD−phenylalanine, respectively. These two orthogonal detection schemes allow analysis of a wider spectrum of compounds per separation, leading to higher throughput and enabling resolution of two neutral analytes, NBD−arginine and catechol. In addition, insight into the detection and separation mechanisms is realized. Differences in migration time and peak widths between the two detectors are compared, providing a better understanding of detector alignment. A common problem encountered in electrophoresis is run-to-run migration time irreproducibility for certain samples. This novel microchip dual detection system has been utilized to reduce this irreproducibility. An unknown sample is monitored with one detector while a standard (i.e., ladder) is added to the sample and monitored simultaneously with the other detector. This dual detection method is demonstrated to normalize unknown peak mobilities in a cerebral spinal fluid sample.

In an effort to generate total analysis systems,[1] there has been considerable development in miniaturization of analytical tools using microfabrication methodologies. The fabrication process has facilitated construction of short separation channels, intricate designs, and functional features, such as valves, reaction and mixing chambers, and detection hardware (see reviews).[2−4] Developments of all aspects of microchip technology are being investigated to expand the applicability of a total analysis device, including increasing sample throughput, which is important when analyzing complex and large numbers of samples. These developments have been focused on multiplexing separation lanes[5−7] and performing ultrafast[8] and orthogonal[9] separations. An aspect of high-throughput chip-based separation systems that has received little attention is multiplexing detection schemes.

Several detection schemes have been developed that could be multiplexed to provide orthogonal information.[10−24] Some of these orthogonal detection schemes have been utilized to gain perspective on detection characterization in microchips. Concern regarding the band broadening observed in mass spectrometric analysis off a microchip led Lazar and co-workers to use fluorescence detection to track dispersion.[25] Recently, Martin et al. used fluorescence detection to characterize the band-broadening and peak-skewing observed in electrochemical (EC) detection on a chip.[26] Although in both of these studies, the detection techniques were not accomplished simultaneously, exploiting orthogonal detection techniques to obtain relevant information was demonstrated.

Multiple detection strategies have been coupled for simultaneous detection on microchips to enhance analysis and increase

† Both authors contributed equally to the work presented herein.

* Fax: (814) 863−8081. E-mail: age@psu.edu.

(1) Manz, A.; Harrison, D. J.; Verpoorte, E.; Fettinger, J. C.; Paulus, A.; Ludi, H.; Widmer, H. M. *J. Chromatogr.* **1992**, *593*, 253−258.
(2) Lacher, N. A.; Garrison, K. E.; Martin, R. S.; Lunte, S. M. *Anal. Chem.* **2001**, *22*, 2526−2536.
(3) Bruin, G. J. M. *Electrophoresis* **2000**, *21*, 3931−3951.
(4) Dolnik, V.; Lui, S.; Jovanovich, S. *Electrophoresis* **2000**, *21*, 41−54.
(5) Simpson, P. C.; Roach, D.; Woolley, A. T.; Thorsen, T.; Johnston, R.; Sensabaugh, G. F.; Mathies, R. A. *Proc. Natl. Acad. Sci.* **1998**, *95*, 2256−2261.
(6) Shi, Y.; Simpson, P. C.; Scherer, J. R.; Wexler, D.; Skibola, C.; Smith, M. T.; Mathies, R. A. *Anal. Chem.* **1999**, *71*, 5354−5361.
(7) Cheng, S. B.; Skinner, C. D.; Taylor, J.; Attiya, S.; Lee, W. E.; Picelli, G.; Harrison, D. J. *Anal. Chem.* **2001**, *73*, 1472−1479.
(8) Jacobson, S. C.; Hergenroder, R.; Kouthy, L. B.; Ramsey, J. M. *Anal. Chem.* **1994**, *66*, 1114−1118.
(9) Grab, B.; Neyer, A.; Johnck, M.; Siepe, D.; Eisenbeib, F.; Weber, G.; Hergenroder, R. *Sens. Actuators B* **2001**, *72*, 249−258.
(10) Harrison, D. J.; Fan, Z. H.; Seiler, K.; Manz, A.; Widmer, H. M. *Anal. Chim. Acta* **1993**, *283*, 361−366.
(11) Jacobson, S. C.; Koutny, L. B.; Hergenroder, R.; Moore, A. W., Jr.; Ramsey, J. M. *Anal. Chem.* **1994**, *66*, 3472−3476.
(12) Woolley, A. T.; Mathies, R. A. *Proc. Natl. Acad. Sci.* **1994**, *91*, 11348−11352.
(13) Ocvirk, G.; Tang, T.; Harrison, D. J. *Analyst* **1998**, *123*, 1429−1434.
(14) Gavin, P. F.; Ewing, A. G. *Anal. Chem.* **1996**, *69*, 3838−3845.
(15) Woolley, A. T.; Lao, K.; Glazer, A. N.; Mathies, R. A. *Anal. Chem.* **1998**, *70*, 684−688.
(16) Henry, C. S.; Zhong, M.; Lunte, S. M.; Kim, M.; Bau, H.; Santiago, J. J. *Anal. Commun.* **1999**, *36*, 305−307.
(17) Xue, Q.; Foret, F.; Dunayevskiy, Y. M.; Zavracky, P. M.; McGruer, N. E.; Karger, B. L. *Anal. Chem.* **1997**, *69*, 426−430.
(18) Ramsey, R. S.; Ramsey, J. M. *Anal. Chem.* **1997**, *69*, 1174−1178.
(19) Figeys, D.; Ning, Y. B.; Aebersold, R. *Anal. Chem.* **1997**, *69*, 3153−3160.
(20) Xu, N.; Lin, Y.; Hofstadler, S. A.; Matson, D.; Call, C. J.; Smith, R. D. *Anal. Chem.* **1998**, *70*, 3553−3556.
(21) Salimi-Moosavi, H.; Jiang, Y.; Lester, L.; McKinnon, G.; Harrison, D. J. *Electrophoresis* **2000**, *21*, 1291−1299.
(22) Nakanishi, H.; Nishimoto, T.; Arai, A.; Abe, H.; Kanai, M.; Fujiyama, Y.; Yoshida, T. *Electrophoresis* **2000**, *22*, 230−234.
(23) Burggraf, N.; Krattiger, B.; de Mello, A. J.; de Rooij, N. F.; Manz, A. *Analyst* **1998**, *123*, 1443−1447.
(24) Walker, P. A., III.; Morris, M. D.; Burns, M. A.; Johnson, B. N. *Anal. Chem.* **1998**, *70*, 3766−3769.
(25) Lazar, I. M.; Ramsey, R. S.; Sundberg, S.; Ramsey, J. M. *Anal. Chem.* **1999**, *71*, 3627−3631.
(26) Martin, R. S.; Ratzlaff, K. L.; Huynh, B. H.; Lunte, S. M. *Anal. Chem.* **2002**, *74*, 1136−1143.

10.1021/ac025504p CCC: $22.00
Published on Web 05/25/2002

throughput by providing additional information. For example, collection of scatter and fluorescence signal has been utilized in a microchip flow cytometry device.[27] This device has been applied to fluorescently labeled *Escherichia coli* to yield information on cell viability and to determine stages of cell division.[28] Similarly, dual detection electrodes held at different potentials have been positioned at the end of the separation channel.[29,30] This EC technique allowed selective detection of reversible electrochemical species, aided in peak identification, and determined recovery rates for the EC reduction reaction.

Since many detectors are selective for a certain chemical characteristic or structural motif, the choice of detection method introduces a fundamental limit to the applicability of the device. Combination of orthogonal detection schemes can be used to accomplish high-throughput analysis and improve sample characterization. Laser-induced fluorescence (LIF) and amperometric detection are generally orthogonal in terms of the analytes that can be detected. LIF is the most widespread chip detection method because of its high sensitivity and ease of coupling with a microchip. Derivatization tags enable specific labeling of analytes, and optical components for fluorescence detection have been miniaturized in a chip device.[31] EC microchip detection is receiving increased attention, because the detection element can be miniaturized on the chip, is sensitive, and provides a means to determine some molecules that are not easily detected by fluorescence. In this paper, LIF and EC detection are employed for simultaneous detection on a chip. The effectiveness of this dual detection system for characterization of separation and detection and its application to normalizing migration times in biological samples is demonstrated.

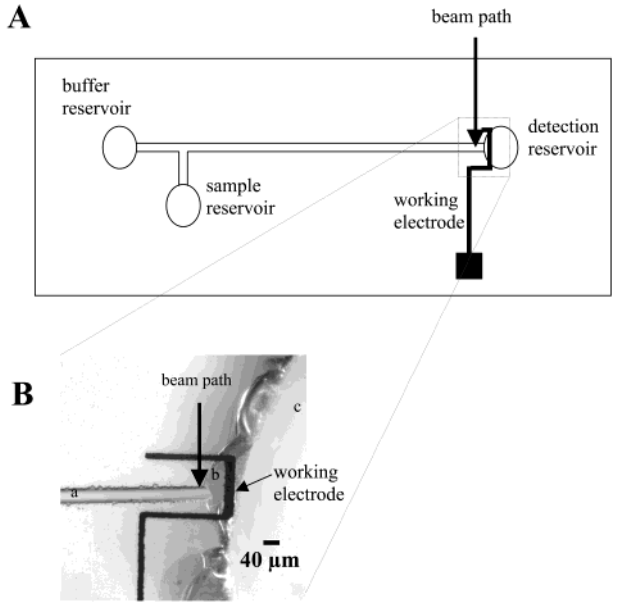

Figure 1. (A) Schematic representation of the functional parts of the microchip employed. The laser beam for LIF detection is placed right at the channel outlet while the detection electrode is aligned ~55 μm away from the etched channel exit. (B) An enlargement of the dual detection region of the microchip is shown. Before bonding, the access hole was drilled, which intersects the (a) etched channel, chipping away a (b) conical channel exit. The detection beam (shown by arrow) is focused to a position just before the point of widening. The thin-film platinum electrode (20 μm wide) was aligned ~55 μm beyond the point of widening and before the (c) bulk reservoir. Separation channel dimensions: 34 μm full-width, 8.4 μm deep, 1.5 cm from tee to detection reservoir, 0.5 cm from tee to buffer and sample reservoirs.

EXPERIMENTAL SECTION

Reagents. Reagents were obtained from Sigma Chemical Co. (St. Louis, MO) unless otherwise noted. TES (*N*-tris(hydroxymethyl)methyl-2-amino-ethanesulfonic acid, 10 mM, pH adjusted to 7.4) and boric acid (10 mM, pH adjusted to 9.2) were prepared for use as run buffers. Stock solutions of NBD (4-chloro-7-nitrobenzofurazan, 20 mM, Molecular Probes, Eugene, OR) in acetone (Burdick & Jackson, Muskegon, MI) and amino acids (20 mM) in borate buffer were prepared. Labeling reagent and amino acid solutions were mixed to yield a 10-fold molar excess of labeling reagent, allowed to react for 15 min, and diluted to the desired concentration with the appropriate buffer.[32] Stock solutions of dopamine (10 mM) and catechol (100 mM) were prepared in 100 mM perchloric acid to prevent oxidation in solution and diluted to the desired concentration with the appropriate buffer.

Microchip Fabrication. The relevant portion of the electrophoresis chip is shown in Figure 1A. The microchip had four reservoirs in a typical cross-tee geometry; however, only three reservoirs were employed. The chips were fabricated in-house at the EMPRL Nanofabrication Facility (Pennsylvania State University, University Park, PA). Corning 2947 soda lime glass plates (VWR, Philadelphia, PA) were cleaned with acetone, 2-propanol, and water and then were dipped in hot piranha etch (3:1 H_2SO_4/H_2O_2). (**Caution:** *piranha etch should be handled with care, since it is a strong oxidizing agent that reacts violently with organic compounds.*)

The separation channel was fabricated using traditional photolithography with a sacrificial metal bilayer. To achieve a smooth etch of the soda lime glass, the substrate was placed feature-side-down in a mixture of 1 part (6:1) buffered oxide etch/2 parts hydrochloric acid/4 parts water while stirring at 250 rpm, producing channel depths of 8−12 μm (adapted from Stjernstrom et al.).[33] Final channel dimensions were determined with a Tencor 500 AlphaStep surface profilometer (KLA-Tencor Corporation, San Jose, CA).

The electrode plate was constructed using rapid prototyping[29,34] at 5080 dpi using a high-resolution image setter (Jostens Inc., State College, PA) and metal lift-off for pattern definition.[35] The electrode pattern was lithographically transferred to the clean soda lime glass employing SPR-1827 photoresist (Shipley Company, Marl-

(27) Schrum, D. P.; Culbertson, C. T.; Jacobson, S. C.; Ramsey, J. M. *Anal. Chem.* **1999**, *71*, 4173−4177.
(28) McClain, M. A.; Culbertson, C. T.; Jacobson, S. C.; Ramsey, J. M. *Anal. Chem.* **2001**, *73*, 5334−5338.
(29) Martin, R. S.; Gawron, A. J.; Lunte, S. M. *Anal. Chem.* **2000**, *72*, 3196−3202.
(30) Gawron, A. J.; Martin, R. S.; Lunte, S. M. *Electrophoresis* **2001**, *22*, 242−248.
(31) Lindner, E.; Buck, R. P. *Anal. Chem.* **2000**, *72*, 336−345.
(32) Fager, R. S.; Kutina, C. B.; Abrahamson, E. W. *Anal. Biochem.* **1973**, *53*, 290−294.
(33) Stjernstrom, M.; Roeraade, J. *J. Micromech. Microeng.* **1998**, *8*, 33−38.
(34) Duffy, D. C.; McDonald, J. C.; Schueller, O. J. A.; Whitesides, G. M. *Anal. Chem.* **1998**, *70*, 4974−4984.
(35) Kovacs, G. T. A. *Micromachined Transducers Sourcebook*; McGraw-Hill Inc.: New York, 1998; 98−100.

borough, MA). Titanium (200 Å) for an adhesion layer and platinum (2000 Å) for the working electrode were evaporated onto the patterned plate. By sonicating in acetone, the photoresist and unwanted metal were removed, revealing the Ti/Pt electrode. The lift-off technique was observed to produce a surface free of residual photoresist and minimized processing of the electrode plate.

Access holes (2-mm diameter) were drilled into the channel plate for sample, buffer, and electrode access. The drilled hole at the detection reservoir served to define the detection region for the electrochemical cell. Drilling the detection reservoir in the channel plate after the channel was etched fortuitously resulted in a chipping away of the channel walls just before the bulk reservoir, forming a conical channel exit.

The channel and electrode plates were cleaned with acetone, 2-propanol, and water before aligning under a light microscope. The working electrode (20 μm wide and ~150 μm in length) was aligned within the conical exit, ~50 μm from the separation channel, in an end-column fashion to isolate the electrode potential from the separation potential, as described for previous EC detection in both capillary[36−39] and microchip electrophoresis.[14−16,29,40] The chip was thermally bonded in an oven (Vulcan 3-130, Ney Dental Inc., Bloomfield, CT) using a temperature program (20 °C/min ramp to 450 °C, 10 °C/min to 600 °C held for 3 h, 10 °C/min ramp to 450 °C, and then allowed to cool to room temperature). After cooling, electrical connection to the working electrode on the microchip was accomplished by attaching a small segment of flexible wire to the microfabricated contact pad with silver epoxy (Epoxies Etc., Cranston, RI).

Instrumentation. The microchip was placed on the stage of an inverted microscope (Olympus, Melville, NY). Platinum electrodes, used to apply electrophoretic potential, were connected to a high-voltage power supply (Bertan, Hicksville, NY). The injection end of the chip was held at a positive potential with respect to the detection end.

Confocal fluorescence detection was performed as described previously.[41] In brief, a 488-nm line (~2 mW) from an argon ion laser (Innova 70, Coherent, Santa Clara, CA) was passed into an inverted microscope (70X Olympus, Melville, NY) that contained a dichroic mirror (Chroma Technology, Brattleboro, VT) and a 20×, 0.4-numerical-aperture microscope objective (Olympus, Melville, NY). The fluorescence signal was spatially (500-μm pinhole, L39-729, Edmund Industrial optics, Barrington, NJ) and optically (51300, Oriel, Stratford, CT and D530/20M, Chroma Technology, Brattleboro, VT) filtered, and gathered with a photomultiplier tube (Hamamatsu, Bridgewater, NJ).

Amperometric detection was performed using a two-electrode cell. A 250-μm-diameter silver wire (Goodfellow, Huntingdon, England), oxidized in 1 M KCl solution, was used as a pseudoreference electrode and placed ~50−100 μm from the working electrode. The working electrode was maintained at +700 mV (vs Ag/AgCl) using a battery-operated floating potentiostat made in-house. The signals from both detectors were then amplified (427, Keithley Instruments, Cleveland, OH), sent to an interface (BNC 2090, National Instruments, Austin, TX) and collected simultaneously at 50 Hz (PCI-MIO 10XE50, National Instruments, Austin, TX) using an in-house program written in Labview (National Instruments, Austin, TX).

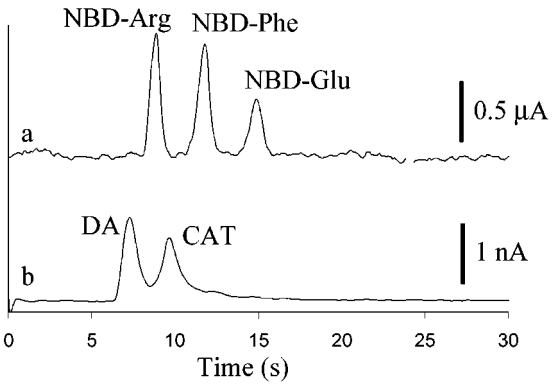

Figure 2. Simultaneous detection of a five-component sample in TES buffer. Electropherograms obtained using (a) LIF and (b) EC dual detection. Peaks are identified as DA (50 μM), CAT (110 μM), and NBD-labeled Arg (140 μM), Phe (180 μM), and Glu (220 μM). Conditions are a 1-s injection and separation at 208 V/cm field strength.

Procedures. Capillary action and a vacuum pump (Welch 8890, Thomas Industry, Skokie, IL) were used to fill the separation channel with solution prior to use. An enlarged view of the detection end of the microchip is shown in Figure 1B. The beam for LIF detection is placed inside the separation channel (~65 μm in front of the electrode) to maximize signal-to-noise and minimize band-broadening of the two detection systems. Sample introduction was performed using a cross-tee configuration in which only three reservoirs were employed: a buffer, sample, and detector reservoirs.[42] Sample was loaded into the separation channel by applying potential between the sample and detector reservoirs, floating the buffer reservoir. The same voltage was used for separation by applying the potential between the buffer and detector reservoirs, floating the sample reservoir.

CSF Samples. Cerebral spinal fluid (CSF) samples from multiple sclerosis patients were obtained from James Landers (currently at the University of Virginia) in Spring 1998 and were stored at −18 °C. Thawed CSF samples were labeled with 2 times v/v ratio of NBD stock and reacted at room temperature in the dark for at least 15 min. Samples were centrifuged (10 s at 5000 rpm), and an aliquot of supernatant was diluted by half with ultrapure water (Milli-Q, Millipore, Bedford, MA). The labeled CSF sample was spiked with electroactive species and placed on the sample reservoir of the chip for analysis.

RESULTS AND DISCUSSION

Characterization of On-Chip Dual Detection. The electroactive analytes dopamine (DA) and catechol (CAT), and fluorescently labeled arginine (NBD−Arg), phenylalanine (NBD−Phe), and glutamic acid (NBD−Glu) have been chosen for study on the basis of their differences in charge and size. A representative electropherogram of these analytes with simultaneous LIF and EC detection is shown in Figure 2. As expected, the first

(36) Huang, X.; Zare, R. N.; Sloss, S.; Ewing, A. G. *Anal. Chem.* **1991**, *63*, 189−192.
(37) Haber, C.; Silvestri, I.; Roosli, S.; Simon, W. *Chimia* **1991**, *45*, 117−121.
(38) Sloss, S.; Ewing, A. G. *Anal. Chem.* **1993**, *65*, 577−581.
(39) Klett, O.; Bjorefors, F.; Nyholm, L. *Anal. Chem.* **2001**, *73*, 1909−1915.
(40) Wang, J.; Tian, B.; Sahlin, E. *Anal. Chem.* **1999**, *71*, 5436−5440.
(41) Lapos, J. A.; Ewing, A. G. *Anal. Chem.* **2000**, *72*, 4598−4602.
(42) Harrison, D. J.; Manz, A.; Fan, Z.; Ludi, H.; Widmer, H. M. *Anal. Chem.* **1992**, *64*, 1926−1932.

compound detected is DA, a cation, with EC detection. The second peak to migrate past the detector is the neutral NBD-labeled Arg, fluorescently detected, followed by the neutral CAT in the EC trace. Then NBD−Phe and NBD−Glu, both low-mobility anions, are detected fluorescenctly. All of the sample components are detected with their respective techniques and have no apparent interference with each other.

Because a standard zone electrophoresis separation is performed, neutrals migrate with electroosmotic flow (EOF) and do not separate. However, the neutrals NBD−Arg and CAT are resolved as a result of the selectivity of these orthogonal detection techniques. The two neutral peaks are expected to be detected simultaneously; however, there is a noticeable time difference in the migration of the neutrals shown in Figure 2 (8.88 and 9.66 s for NBD−Arg and CAT, respectively). On the basis of simple diffusion calculations, the time for analytes to diffuse from the channel outlet to the electrochemical detector is ∼3.0 s. In contrast, the time for EOF to traverse this distance is estimated to be 0.038 s. The experimentally measured time for analytes to move between the outlet (location of the fluorescence probe beam) and the amperometric electrode was 0.76 s. Thus, visual observation of the flow of a fluorescent plug at the channel outlet was employed to better understand fluid movement at the channel outlet. The fluorescent analyte zone was observed to spread at a consistent dispersion angle as the sample collected at the channel exit (data not shown). Utilizing this spreading profile, the analyte volume at the detection reservoir has been calculated. Because volume flow rates are conserved between the etched channel and the channel exit, times of 0.5, 0.9, and 1.2 s were needed for an analyte to travel from the LIF beam to the front, middle, and back of the electrode, respectively. The experimentally observed migration time-shift value of the neutral analytes in Figure 2 corresponds to maximum detection occurring between the front and middle of the electrode.

The dispersion effects at the end of the separation channel also may account for the difference in peak widths between the two traces (Figure 2). The EC peaks are 2.5 times wider than those in the fluorescence trace run simultaneously. In addition, there is increased asymmetry of peaks from end-column detection. This asymmetry can likely be attributed to the slowing of the fluid flow as it crosses the electrode width and to the diffusion-limited nature of the detector. Therefore, the EC peaks show more tailing than the LIF peaks. Broad, tailed peaks have been observed previously for EC detection and investigated. Work by Martin et al. reveals improved peak shape when in-channel EC detection is performed, as opposed to end-column detection.[26] These results were attributed to the minimal dispersion and smaller exposed electrode area of the in-column detector. The results obtained with the simultaneous detection reported in this paper support those obtained previously with the in-channel detector.

Characterization of On-Chip Separations. Experimental parameters were investigated to ensure optimal separation with the dual detection scheme. Shown in Figure 3 are electropherograms obtained at different injection times. Electrokinetic injections have been known to preferentially load high mobility analytes.[30] Thus, more DA, a cation, is loaded, as compared to anions, such as NBD−Phe and NBD−Glu. While adequately loading low mobility analytes, longer injection times cause the

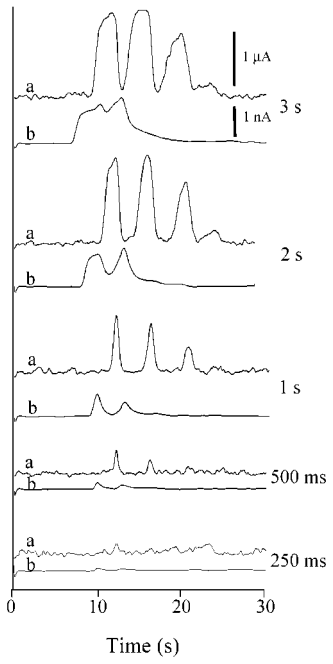

Figure 3. Effect of injection time on (a) LIF and (b) EC dual detection of a five-component sample. Conditions, except for injection time, are the same as in Figure 2.

efficiency and resolution of the separation to be sacrificed. The best separations are obtained with a 1-s injection time for the analytes used here. At this injection time, all analytes are adequately loaded while optimizing efficiency (plate heights of 3.2−7.6 μm for the fluorescent analytes and 14.6 μm and 30.4 μm for the electroactive analytes) and resolution ($R = 1.05$ between DA and CAT) of the separations. Various injection schemes for EC detection on chips[15,30,43] are being considered for future work to maintain the detection reservoir at ground but reduce the preferential loading.

The effect of run voltage on the separation outcome was also investigated, and the results are presented in Figure 4. A comparison of a 1-s injection at each of the different field strengths demonstrates that, as expected, migration time decreases as the field strength increases. Because of the nature of the injection method, more sample is loaded at the higher field strengths (396 pL at 208 V/cm vs 582 pL at 310 V/cm), which causes the resolution of DA and CAT in the EC trace to be compromised. A calibration of the two detection techniques utilizing a 1-s injection time and a 208 V/cm field strength in TES buffer demonstrates a linear response for both the fluorescent ($r^2 = 0.98$ for NBD−Arg; $r^2 = 0.992$ for NBD−Phe over a range of 12.5 μM to 1 mM) and electroactive ($r^2 = 0.994$ for DA over a concentration range of 0.5 to 50 μM; $r^2 = 0.98$ for CAT over a concentration range of 2−200 μM) analytes. The limit of detection was calculated to be 448 nM and 1.52, 16, and 28 μM for DA, CAT, NBD−Arg, and NBD−Phe, respectively. (The low mobility of NBD−Glu results in poor loading during injection. Thus, low concentrations of NBD−Glu were not detected, and not enough data points were obtained to evaluate its detection limit.) These detection limits are comparable to those observed in microchips for these analytes with their respective detection techniques.[30,40,41]

(43) Liu, Y.; Joseph, C. F.; Bledsoe, J. M.; Henry, C. S. *Anal. Chem.* **2000**, *72*, 5939−5944.

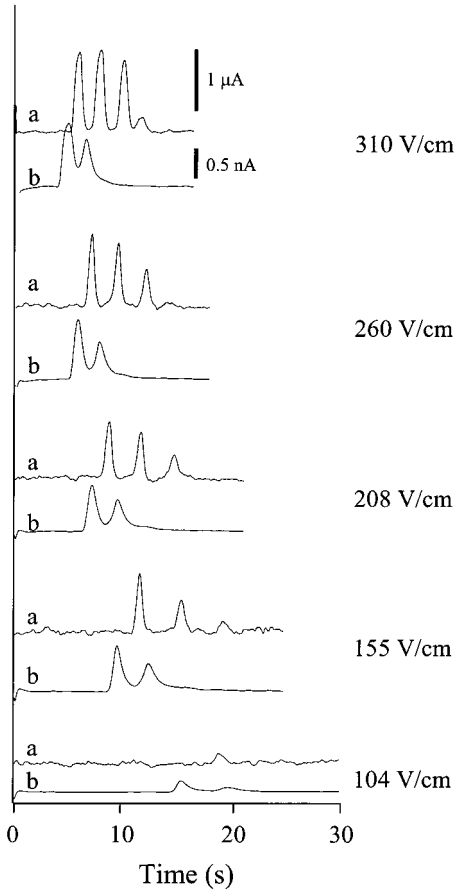

Figure 4. Effect of field strength on (a) LIF and (b) EC dual detection of a five-component sample. The fourth peak in the fluorescence trace is attributed to an impurity in the Arg sample, most likely the result of double labeling. Conditions, except for field strength, are the same as in Figure 2.

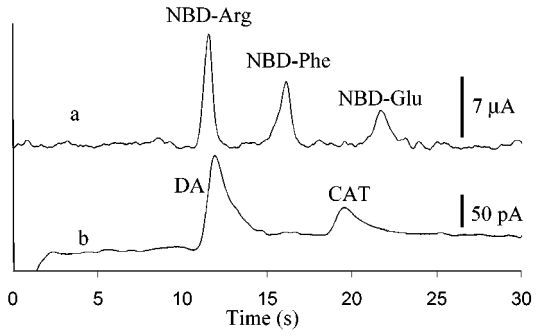

Figure 5. Simultaneous (a) LIF and (b) EC dual detection of a five-component sample in borate buffer. Peaks identified as DA (100 μM), CAT (930 μM), and NBD-labeled Arg (150 μM), Phe (340 μM), and Glu (350 μM). Other conditions are identical to Figure 2.

Valuable information regarding the separation can be attained when combining two detection methods with a single microchip separation.[27−30] A separation was performed under identical conditions with two different run buffers: TES (Figure 2) and borate (Figure 5). Comparison of the LIF and EC traces in the two electropherograms shows a noticeable change in the migration order. This shifting of the migration order is a result of the complexation of the catechols with tetrahydroxyborate anions

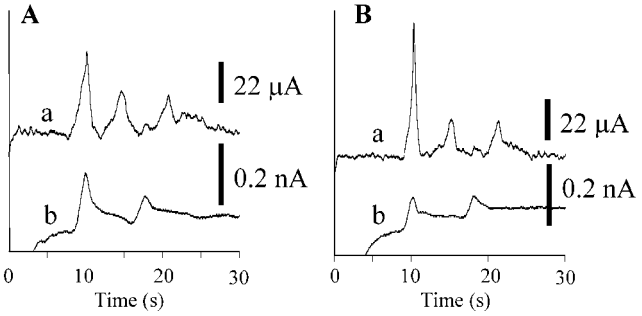

Figure 6. Simultaneous (a) LIF and (b) EC dual detection of fluorescently labeled CSF samples from two unknown patients, labeled (A) and (B) here, and spiked with electrochemically active DA (50 μM) and CAT (1 mM). Conditions are 2-s injection at 208 V/cm and separation at 310 V/cm with 10 mM borate run buffer.

formed in the borate run buffer.[44,45] Thus, DA, a cation in TES buffer, acquires an added negative charge from the borate complex, rendering it a zwitterion, and CAT becomes an anion.

The potential for using dual detection to assist in sample characterization is illustrated by the comparison of Figures 2 and 5. Assuming the fluorescence trace is the standard in both figures, where NBD−Arg is a neutral marker, inspection of the electrochemical trace immediately shows the migration shift of DA and CAT. In these experiments, the fluorescence trace can be thought of as an internal standard that does not interfere with EC detection and can be used to evaluate migration order changes of the electroactive compounds as they are complexed with the borate. Combining two detection methods in a single separation has several advantages over performing two discrete separations with different detectors. These include faster processing of separation data, more accurate comparisons between traces in the same separation run, and variations in run-to-run elution times can be readily evaluated.

Dual Detection for Peak Normalization. A generally accepted problem in CE is irreproducibility of migration times between runs, leading to questions about peak identification. To aid in peak identification, samples are routinely spiked for comparison. In biological samples, such as CSF, this irreproducibility is especially problematic as a result of the complex sample matrix. CSF is secreted by the brain and functions to cushion the brain and spinal cord from sudden movements and has both a nutritional and immunological function. Because CSF circulates through the central nervous system and is in chemical equilibrium with the neurons and glia, its composition can be used as an indicator of disease.[46,47] Simultaneous LIF and EC detection on a microchip has been applied here to the analysis of CSF samples from two unknown patients (Figure 6). The CSF samples were fluorescently derivatized and then spiked with electroactive components. In this experiment, the EC trace acts as an internal standard, and the fluorescence trace monitors the labeled amines

(44) Steinberg, H. *Organoboron Chemistry*; John Wiley & Sons Inc.: New York, 1964; Chapter 6.
(45) de Jong, J.; Van Alkenburg, C. F. M.; Tjaden, U. R. *J. Chromatogr.* **1985**, *322*, 43−53.
(46) Bergquist, J.; Gilman, S. D.; Ewing, A. G.; Ekman, R. *Anal. Chem.* **1994**, *66*, 3512−3518.
(47) Sanders, E.; Katzmann, J. A.; Clark, R.; Oda, R. P.; Shihabi, Z.; Landers, J. P. *Clin. Chem. Lab. Med.* **1999**, *37*, 37−45.

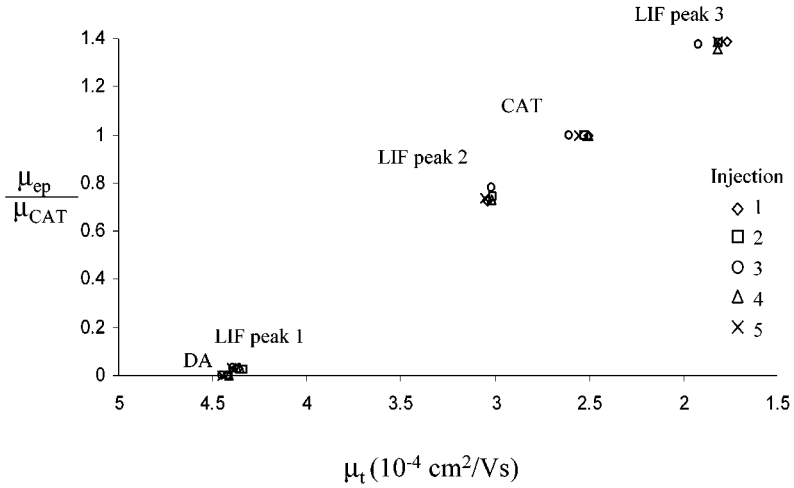

Figure 7. Normalized electrophoretic mobility versus total mobility for five injections of fluorescently labeled sample (Figure 6A) spiked with DA (50 μM) and CAT (1 mM). LIF peak mobilities were normalized to the mobility of CAT for each separation. The five clusters of data points on the graph represent (from left to right) DA, LIF peak 1, LIF peak 2, CAT, and LIF peak 3.

in the sample. These two CSF samples have similar fluorescent peak profiles. Although the migration times of the peaks are similar, often there is difficulty in assessing peak identities.

Employing dual detection enables normalization of analyte peaks between separations to account for shifts in mobility. In capillary electrophoresis, separation of analytes is defined by the differential mobility. The total mobility of a compound (μ_t) is the sum of its electrophoretic mobility (μ_{ep}) and eletroosmotic mobility (μ_{EOF}, which is indicated by the neutral analyte) by the equation

$$\mu_t = \mu_{ep} + \mu_{EOF}$$

A spiked CSF sample was injected and the migration times for the three main LIF peaks observed were used to determine μ_t. The focus of the CSF analysis is to describe potential application of dual detection as a method of normalizing run-to-run variations. Exact identification of the three LIF peaks was not performed; however, on the basis of previous work in capillaries, the three LIF peaks can be attributed to neutral species, unresolved γ and β immunoglobulin regions, followed by albumin.[48] Because DA is complexed with borate and has a net neutral charge, it is used as a marker for EOF, and this value is used to calculate the μ_{ep} for each of the three LIF peaks and CAT. The μ_{ep} of each LIF peak is normalized to the μ_{ep} of CAT detected amperometrically and plotted vs μ_t in Figure 7. Employing two (or more) internal standard markers that span the peaks of interest is advantageous, as illustrated in Figure 7. These internal standards can act as a ruler or a ladder upon which the unknowns can be measured. The run-to-run variation in the data for each LIF peak is reduced when mobilities are normalized to the electrochemical signal. This is observed in the relatively tight clustering of normalized mobilities (μ_{ep}/μ_{CAT}) vs raw mobilities (μ_t) for peaks in five repeated separations. For example, LIF peak 3 has a 2.7% relative standard deviation in μ_t and only 0.82% relative standard deviation after normalization. Because the internal standards, DA and CAT, are both employed as an "invisible ladder", unknown peaks can be normalized between separate samples and separate days to account for variability in migration times.

(48) MacTaylor, C. E., Pennsylvania State University, 1998.

CONCLUSION

Simultaneous LIF and EC detection has the ability to increase throughput by detecting analytes with different physical characteristics. The orthogonal nature of the two detection schemes enables the detection of neutral markers within their respective techniques with no apparent interference between the two detectors. Use of two simultaneous detectors provides opportunities to optimize performance for both detection and separation. It should be possible through optimization to obtain detection limits with microchips similar to those achieved in capillaries. Information about a given separation is available with simultaneous dual detection, such as that shown in the complexation of catechols with borate buffer. Variation in migration times is minimized with these methods, and normalization of complex sample separations with the use of standard ladders is demonstrated. Application of dual detection for quantitative analysis with internal standards can be envisioned. Additionally, because cells contain chemically diverse species, dual LIF and EC detection could be exploited to achieve more information for high-throughput cell analysis.

ACKNOWLEDGMENT

Funding for this research was provided by the National Science Foundation. The authors thank James Landers from the University of Virginia for the CSF samples and the following people for assistance in conversion of mask files to true-scale high-resolution films: Ash Parameswaran of Simon Fraser University, Rajib Ganguly and Michele Stark of Pennsylvania State University, and Karen Nichols at Jostens, State College, PA. The chip fabrication was performed in part at the Penn State Nanofabrication Facility, a member of the National Nanofabrication Users Network, which is supported by the National Science Foundation under Grant No. 33810-6190, The Pennsylvania State University, and industrial affiliates.

Received for review January 4, 2002. Accepted April 18, 2002.

AC025504P